CHEMISTRY OF MATERIALS

Article

pubs.acs.org/cm

Insights into Changes in Voltage and Structure of Li_2FeSiO_4 Polymorphs for Lithium-Ion Batteries

C. Eames,[†] A. R. Armstrong,[‡] P. G. Bruce,[‡] and M. S. Islam*[,†]

[†]Department of Chemistry, University of Bath, BA2 7AY, United Kingdom

[‡]School of Chemistry, University of St. Andrews, Fife, KY16 9ST, United Kingdom

Supporting Information

ABSTRACT: The search for new low cost, safe, and high capacity cathodes for lithium batteries has focused attention recently on Li_2FeSiO_4. The material presents a challenge because it exhibits complex polymorphism, and when it is electrochemically cycled there is a significant drop in the cell voltage related to a structural change. Systematic studies based on density functional theory techniques have been carried out to examine the change in cell voltages and structures for the full range of Li_2FeSiO_4 polymorphs (β_{II}, γ_s, and γ_{II}) including the newly elucidated cycled structure (termed inverse-β_{II}). We find that the cycled structure has a 0.18−0.30 V lower voltage than the directly synthesized polymorphs in accord with experimental observations. The trends in cell voltage have been correlated to the change in energy upon delithiation from Li_2FeSiO_4 to $LiFeSiO_4$ in which the cation−cation electrostatic repulsion competes with distortion of the tetrahedral framework.

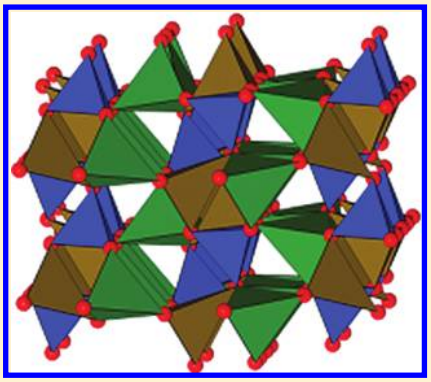

KEYWORDS: *lithium battery, cathode, silicates, computer simulation, electronic structure*

INTRODUCTION

The next generation of lithium batteries for use in electric vehicles and in large scale storage of renewable energy requires new electrode materials that are low cost, safer, and have a high capacity. One group of materials under investigation is polyoxyanion compounds in which the strong binding of oxygen gives greater thermal stability than in the transition metal oxides. Recently attention has been focused on lithium iron silicate[1−21] (Li_2FeSiO_4), a polyoxyanion compound that offers a cathode made from iron and silicon which are abundant and inexpensive materials.

The Li_2MSiO_4 (M = Fe, Mn, Co) compounds are members of a large family of structures comprised of tetragonally packed oxide ions (a distorted form of hexagonal close packing) in which half of the tetrahedral sites are occupied by cations. The cation site ordering can vary, and the tetrahedra can be distorted giving rich and complex polymorphism.

Several structures have been proposed to describe Li_2FeSiO_4 (shown in Figure 1). The first was reported by Nyten et al.[1] who suggested an orthorhombic structure (based on β-Li_3PO_4), with space group $Pmn2_1$. In this β-structure, chains of LiO_4 tetrahedra run along the a direction parallel to chains of alternating FeO_4 and SiO_4 tetrahedra. Nishimura et al.[5] reported the structure of Li_2FeSiO_4 prepared at 800 °C and designated by these authors as γ_s (space group $P2_1$). It differs from the other γ structures in that there are no edge sharing trimers of tetrahedra; instead one set of LiO_4 tetrahedra are arranged in edge sharing pairs with FeO_4 tetrahedra, while the other set of LiO_4 tetrahedra forms edge sharing pairs with itself. More recently this description has been simplified using the higher symmetry space group $P2_1/n$.[6] Sirisopanaporn et al.[7] have recently described the crystal structure of a new γ_{II}-polymorph of Li_2FeSiO_4, obtained by quenching from 900 °C that differs from the γ_s structure obtained by quenching from 800 °C. Li_2FeSiO_4 can be prepared by a variety of synthetic routes. These include hydrothermal synthesis which gives rise to the ordered β_{II} polymorph (space group $Pmn2_1$),[5,9,19] while other higher temperature procedures produce the γ_s form (space group $P21/n$).[2]

The as-prepared structures, and as a result the voltage and polarization of this cathode, change during the first few cycles, then remain constant;[8] the observed drop in cell voltage vs Li^+/Li is of the order 0.18−0.30 V.[4,8,9] Only very recently has the structure of cycled Li_2FeSiO_4 been elucidated,[10] which differs significantly from the as-prepared form. In the ideal β_{II} structure, Li^+ and Fe^{2+} occupy different crystallographic sites, whereas in the cycled structure the site normally occupied by Fe^{2+} is occupied exclusively by Li^+, with the remaining Li^+ sharing the conventional Li site with the Fe ions. This structure is essentially the same as that adopted by the β_{II} polymorph of Li_2CoSiO_4 and is somewhat analogous to the relationship between normal and inverse spinels; hence, the cycled polymorph of Li_2FeSiO_4 has been labeled as inverse-β_{II} (space group $Pmn2_1$).[10]

Due to this complex polymorphism, the factors behind the voltage differences between the polymorphs at the local

Received: March 8, 2012
Revised: May 2, 2012
Published: May 23, 2012

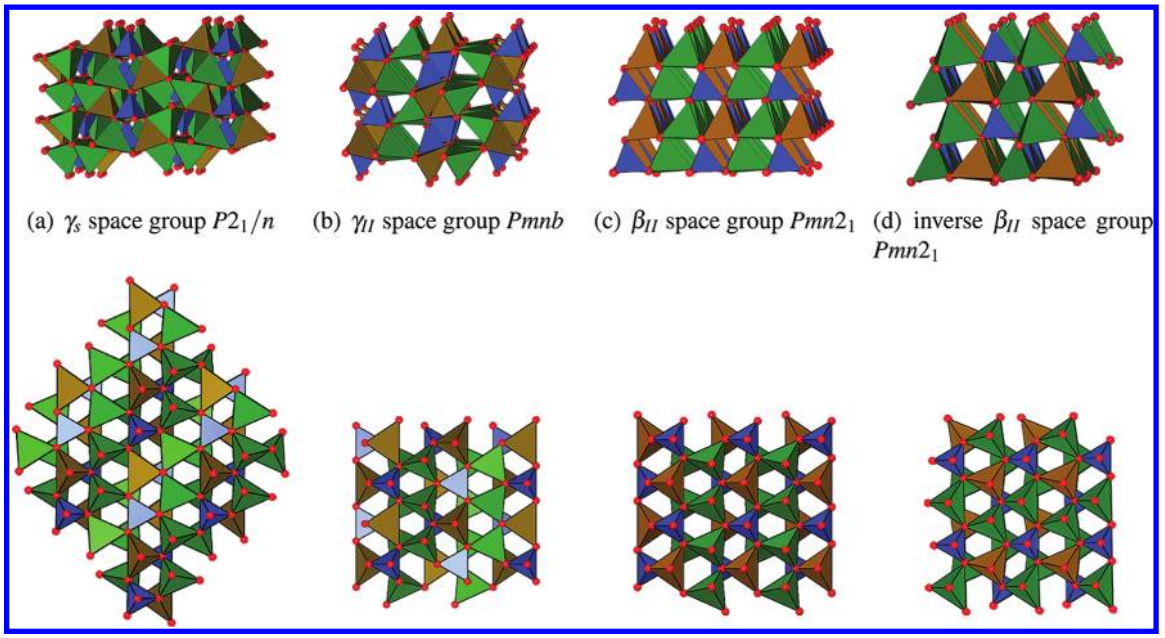

Figure 1. Structures of Li_2FeSiO_4 polymorphs showing two orthogonal views. (a) γ_s structure (space group $P2_1/n$), in which half of the tetrahedra point in opposite directions and contain pairs of LiO_4/FeO_4 and LiO_4/LiO_4 edge-sharing tetrahedra; (b) γ_{II} structure ($Pmnb$) in which the group of three edge-sharing tetrahedra consist of the sequence Li−Fe−Li; (c) β_{II} structure ($Pmn2_1$) in which all the tetrahedra point in the same direction, perpendicular to the close-packed planes, and share only corners with each other; chains of LiO_4 along the *a*-axis parallel to chains of alternating FeO_4 and SiO_4; and (d) inverse-β_{II} structure ($Pmn2_1$) in which all tetrahedra point in the same direction along the *c*-axis and are linked only by corner-sharing. SiO_4 tetrahedra are isolated from each other, sharing corners with LiO_4 and $(Li/Fe)O_4$ tetrahedra. Key: SiO_4 (blue); FeO_4 (brown); LiO_4 (green); oxygen ions (red).

structural level are not fully understood and are important in any future optimization of Li_2FeSiO_4 as a cathode for Li-ion batteries. The present study uses computational techniques based on density functional theory (DFT) to investigate, at the atomic level, key issues related to the changes in Li_2FeSiO_4 structure and the cell voltage drop on electrochemical cycling, with reference to experimental data where possible. For instance, we examine the hypothesis that the cell voltage is related to the Fe−O bond length and the energetics of the redox couple.[9] Such DFT techniques have been applied successfully to analogous studies of other materials for lithium batteries.[22−25] This study also extends our recent computational studies of defect chemistry and lithium ion transport in Li_2MnSiO_4 and $LiFePO_4$ cathode materials.[26−29]

METHODS

All of our calculations were performed within the framework of density functional theory using the plane wave code CASTEP.[30] Since we require optimized lattice parameters the basis set was converged against the stress which is more sensitive to an under-converged basis set than the forces. A cutoff energy of 700 eV with a k-point mesh density of at least 0.04 $Å^{-1}$ was needed to adequately converge the stress. We used ultrasoft pseudopotentials generated using the internal on-the-fly scheme which makes tailored pseudopotentials for the system and takes care of the nonlinear core correction for iron. A ferromagnetic ordering of the moments on the Fe atoms was found to be lower in energy than an antiferromagnetic ordering, in agreement with the previous DFT work on the silicates.[15−21] Exchange and correlation were treated using the PW91[31] form of the generalized gradient approximation. DFT+U was used to correct the interactions inside the iron d-orbitals with an effective Hubbard U = 4.0 eV which is based on previous work on Fe−silicates and related Fe-based cathode materials. Ceder et al. have self-consistently calculated[32] U for $LiFePO_4$ and olivine $LiFeSiO_4$ to be in the range 4−5 eV, and subsequent DFT studies on the lithium iron orthosilicates have used values in this range. de Dompablo et al. have found[15] that in lithium iron silicate a change in U from +4 eV by ±1 eV causes a small change in voltage by around ±0.13 V. We should emphasize that the focus of this work is understanding the trends in voltage differences which are not affected by the precise magnitude of the Hubbard U term.

Previous DFT studies on a variety of oxide electrode materials[22,33,34] have shown that such methods are well suited to probing lithium insertion/extraction properties and to predicting precise trends in cell voltages. For each polymorph we have calculated the open circuit voltage using

$$V = \frac{\varepsilon(Li_2FeSiO_4) - \varepsilon(Li_xFeSiO_4) - (2-x)\mu(Li)}{2-x} \quad (1)$$

where $\varepsilon(Y)$ is the total energy of material Y and x is the number of lithium atoms per formula unit that have been removed. The calculated cell voltage is then an average over the range of x. In practice we have removed one lithium atom pfu to produce the end member $LiFeSiO_4$. Metallic lithium was used to calculate the chemical potential of a single lithium atom $\mu(Li)$ which is standard practice for cell voltage calculations. To derive the cell voltage for each polymorph we have optimized the Li_2FeSiO_4 and $LiFeSiO_4$ structures and used their minimized energies in eq 1. Various configurations of lithium positions of delithiated $LiFeSiO_4$ were considered for each polymorph with the lowest energy structure used in these calculations.

RESULTS AND DISCUSSION

Bulk Structures and Cell Voltages. Structural optimization of all the Li_2FeSiO_4 polymorphs was performed based on the crystal structures observed experimentally. The calculated and experimental structural parameters for the as-prepared polymorphs (β_{II}, γ_s, and γ_{II}) are compared in Table 1 and show general good agreement, as found in other DFT studies.[15−18,20,21]

As noted, the cycled structure has been derived recently from neutron diffraction by Armstrong et al.[10] We have taken this experimentally derived structure as the starting point for our structure optimizations. It was first necessary to consider how

dx.doi.org/10.1021/cm300749w | *Chem. Mater.* 2012, 24, 2155−2161

Table 1. Calculated and Experimental Lattice Parameters of Three Polymorphs of As-Prepared Li_2FeSiO_4

phase	method	a, b, c (Å)	α, β, γ (deg)
β_{II} ($Pmn2_1$)	DFT+U	6.259, 5.402, 5.027	90.0, 90.0, 90.0
	Expt[9]	6.270, 5.345, 4.962	90.0, 90.0, 90.0
γ_s ($P2_1/n$)	DFT+U	8.265, 5.130, 8.256	90.0, 98.7, 90.0
	Expt[9]	8.231, 5.022, 8.232	90.0, 99.3, 90.0
	Expt[5]	8.229, 5.020, 8.233	90.0, 99.2, 90.0
γ_{II} ($Pmnb$)	DFT+U	6.284, 10.740, 5.175	90.0, 90.0, 90.0
	Expt[9]	6.286, 10.660, 5.037	90.0, 90.0, 90.0

the Li/Fe ions that share a site in the cycled structure (inverse-β_{II}) might order. Diffraction data show no evidence for long-range order, so any order must extend over only limited distances. Different configurations of the shared $(Li/Fe)O_4$ sites were considered. For a P1 supercell there are three permutations of the two Li−Fe−Li−Fe rows in the unit cell. We have optimized supercells with these three mixing schemes, and we find that alternation such that adjacent rows in the unit cell are out of step (Li−Fe/Fe−Li) is favored over in-step alternation (Li−Fe/Li−Fe).

Optimized cell parameters are given in Table 2 along with the relative energies of the three configurations. The optimized

Table 2. Lattice Parameters of Cycled Li_2FeSiO_4 (Inverse-β_{II}) for Different Cation Ordering Schemes[a]

scheme	a, b, c (Å)	α, β, γ (deg)	ΔE (meV)
LiLi‖FeFe	6.080, 5.583, 5.002	90.9, 90.0, 90.0	+480
LiFe‖LiFe	6.396, 5.412, 4.969	90.0, 90.0, 89.5	+216
LiFe‖FeLi	6.258, 5.455, 5.047	90.0, 90.7, 90.0	+0.0
Expt[10]	6.236, 5.423, 4.988	90.0, 90.0, 90.0	

[a]The values determined by powder neutron diffraction are provided for comparison.

structure with the lowest energy gives the best agreement with the experimentally determined lattice parameters (for the atomic positions see the Supporting Information). The minor discrepancies are possibly due to the calculated configuration of the shared $(Li/Fe)O_4$ site in the cycled structure. Nevertheless, the reproduction of these relatively complex structures is not a trivial task and gives us confidence that the simulation methods can be used reliably in the cell voltage calculations.

In Table 3 we compare the experimentally measured cell voltages for all four polymorphs with those calculated in this work and we have also included a comprehensive list of values from elsewhere in the literature. The voltage change upon cycling was obtained by subtracting the cell voltage of the cycled structure from the cell voltage of each of the as-prepared polymorphs.

For the β_{II} phase we calculate the voltage change to be −0.30 V versus measured values of −0.30 and −0.34 V. For γ_s we obtained −0.24 V vs −0.24 V measured and for γ_{II} −0.18 V vs −0.14 V measured. The accuracy in our reproduction of the voltage change (ΔV) on cycling is due to our use of the recently determined cycled structure and a fully stress converged basis set. The absolute values of the cell voltages are around 0.3 V greater than measured, which is a known feature of cell voltage calculations caused partly by the Li−metal reference anode that is used.

Recent DFT work of Saracibar et al.[21] has examined the energetics and electrochemistry of Li_2FeSiO_4, indicating that all

Table 3. Calculated and Experimental Cell Voltages (in volts and vs Li^+/Li) for As-Prepared (V_{AP}) and Cycled (V_{CY}) Li_2FeSiO_4 Structures and Voltage Drop on Cycling (ΔV)[a]

V_{AP}	V_{CY}	ΔV	method	reference
		(a) β_{II}-phase ($Pmn2_1$)		
3.10	2.80	−0.30	Expt	Nyten[8]
3.10	2.76	−0.34	Expt	Sirisopanaporn[9]
3.16			DFT+U	Dompablo[15]
2.66			DFT	Larsson[17]
2.40			DFT	Kohalj[18]
2.60			DFT	Wu[20]
3.30			DFT+U	Wu[20]
3.12	2.83	−0.29	DFT+U	Saracibar[21]
3.34	3.04[b]	−0.30	DFT+U	**this work**
		(b) γ_s-phase ($P2_1/n$)		
3.00	2.76	−0.24	Expt	Sirisopanaporn[9]
3.28			DFT+U	Zhong[16]
3.09	2.83	−0.26	DFT+U	Saracibar[21]
3.28	3.04[b]	−0.24	DFT+U	**this work**
		(c) γ_{II}-phase ($Pmnb$)		
2.90	2.76	−0.14	Expt	Sirisopanaporn[9]
3.22	3.04[b]	−0.18	DFT+U	**this work**

[a]In addition to results from this work, we include a comprehensive list of previous experimental and theoretical data. [b]Cycled structure, inverse-β_{II} phase.[10]

the polymorphs have very similar electrode characteristics in terms of voltage and electronic structure, with the stability of delithiated polymorphs controlled by the strong repulsions between Fe^{3+} (or Fe^{4+}) and Si^{4+} cations. They also find that removal of the second lithium occurs at too high a voltage and causes severe structural distortions.

It is known that in the lithium iron silicates the redox couple $Fe^{2+}-Fe^{3+}$ leads to shorter Fe−O bonds on lithium extraction[15,16] (where of course the charges on Fe represent formal valence states and not actual charges). The cell voltages in the silicates have been related to the strength of the redox couple[9] where it is suggested that shorter average Fe−O bond lengths (with higher Fe−O covalency) and a greater degree of distortion of FeO_4 tetrahedra result in a higher Fe^{2+}/Fe^{3+} redox energy. If the redox couple were solely responsible for the different cell voltages in the polymorphs then the Fe−O bond lengths should follow the same trend as the cell voltages. Following the discussion of Goodenough and Kim,[35] the energy of the redox couple depends not only on the formal valence state of the transition metal ion but also on the covalent component of the cation−anion bonding, which is influenced by the placement and character of any counterion or polyanion and by the Madelung energy of the ionic component of the bonding, which is, in turn, influenced by the bulk structure.

Table 4 presents the calculated cation−oxygen bond lengths and ion−ion separations in the structures of Li_2FeSiO_4 and the delithiated $LiFeSiO_4$. We can see that there is no major trend in the Fe−O bonds other than how they become shorter upon delithiation, suggesting that the energy required to oxidize the Fe^{2+} atoms is not the dominant contribution to the difference in the cell voltages.

Energetics and Voltage Trends. To understand the pattern of cell voltages for the iron silicate polymorphs we must again return to eq 1, which suggests that the cell voltage is proportional to the change in energy upon delithiation (where the lithium metal chemical potential is a constant). This is

dx.doi.org/10.1021/cm300749w | Chem. Mater. 2012, 24, 2155−2161

Table 4. Calculated Mean Cation−O Bond Lengths and Cation−Cation Separations in All Four Polymorphs of Lithium Iron Silicate When in the Delithiated $LiFeSiO_4$ and Lithiated Li_2FeSiO_4 States[a]

	Li_2FeSiO_4				$LiFeSiO_4$			
separation/bond length (Å)	i-β_{II}	β_{II}	γ_s	γ_{II}	i-β_{II}	β_{II}	γ_s	γ_{II}
Li−O	2.06	2.03	2.00	2.01	2.13	2.07	2.05	2.05
Fe−O	**2.05**	**2.06**	**2.05**	**2.05**	**1.92**	**1.93**	**1.92**	**1.91**
Si−O	1.65	1.65	1.65	1.65	1.64	1.65	1.64	1.64
O−O	2.99	2.98	3.10	3.08	2.97	2.88	3.05	2.99
Li−Li	3.10	3.16	2.97	3.11	4.69	4.42	3.42	4.08
Li−Fe	3.16	3.15	2.80	3.03	3.28	3.20	3.20	3.14
Fe−Fe	4.49	4.45	4.12	4.14	4.75	4.31	4.06	4.01
Fe−Si	3.14	3.14	3.14	3.12	3.15	3.09	3.10	3.12

[a]In each state the Fe−O bond lengths are constant across the four polymorphs (highlighted in bold). The inverse-β_{II} polymorph has the largest cation−cation spacings after delithiation.

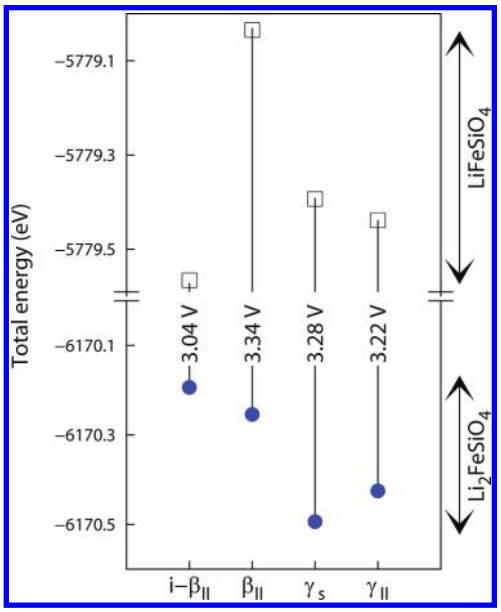

Figure 2. Calculated total energy in the lithiated (Li_2FeSiO_4) and delithiated ($LiFeSiO_4$) state for all four polymorphs together with the calculated cell voltages. The cell voltage is proportional to the energy change upon removal of lithium. Inverse-β_{II} is labeled as i-β_{II}.

illustrated in Figure 2 where the energy of each polymorph is plotted before and after Li removal. We must consider the relative energetics of the polymorphs before and after delithiation and how this correlates with the atomic and electronic structure and the nature of the bonding in each polymorph.

Figure 3 shows the changes in orbital overlap for the Li−O, Fe−O, and Si−O bonds for each of the four polymorphs as Li_2FeSiO_4 and $LiFeSiO_4$. These are derived from Mulliken analysis of the electronic structure.[36] Upon Li extraction from Li_2FeSiO_4 the Fe−O bonds show a clear change in all cases, whereas there is only a very slight change for the Si−O bonds. In the Li−O bonds there is a change upon Li removal (but not in the γ_s structure). Figure 3 therefore indicates significant changes in the Fe−O orbital overlap (and hence in the Fe(3d)−O(2p) mixing) as a result of lithium extraction from the Li_2FeSiO_4 lattice. To be clear our results do not say that the Fe−O bonds become more ionic. The bond population decreases, and there is a change in the electronic structure, which causes the bonding orbitals to shift down in energy, the antibonding orbitals to move up in energy (see Figure 5), and the bond length to become shorter.

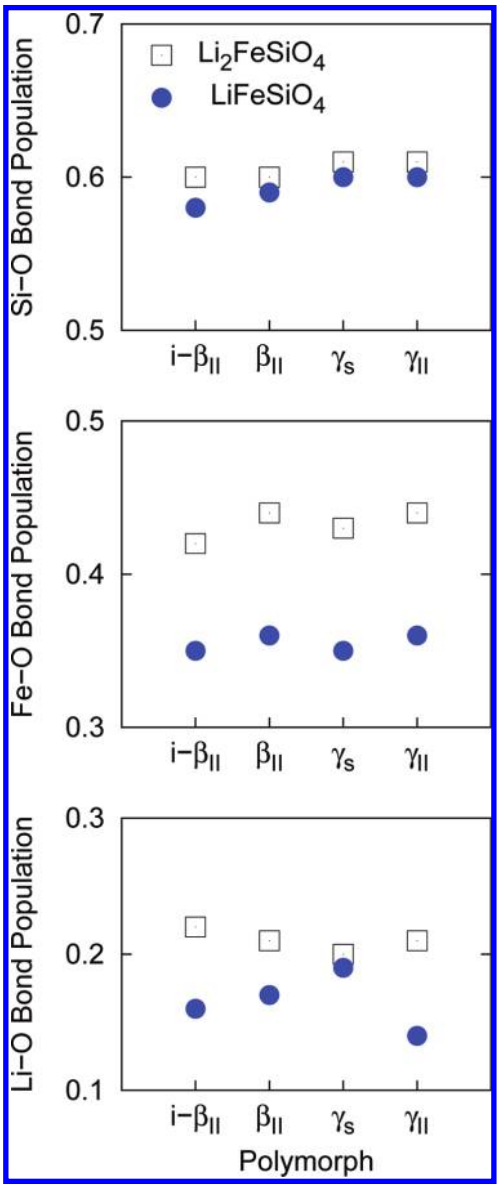

Figure 3. Mulliken bond population in the lithiated (Li_2FeSiO_4) and delithiated ($LiFeSiO_4$) state for all four polymorphs.

The Mulliken analysis also reveals that the atomic populations for Li, Fe, Si, and O also change upon Li extraction (by around +0.18e, +0.36e, +0.10e, and +0.00e, respectively), making all of the cations more positively charged and increasing

dx.doi.org/10.1021/cm300749w | Chem. Mater. 2012, 24, 2155−2161

the cation−cation repulsive energy (see Supporting Information for detailed Mulliken charges). The decreased ionic radius will also contribute to the shortening of the Fe−O bonds.

Thus, in each polymorph there is increased cation−cation repulsion upon Li extraction which acts to increase the volume of the unit cell. At the same time the FeO_4 tetrahedra contract as the Fe−O bonds shorten. These competing effects lead to distortion of all the tetrahedra.

Figure 4 shows the range of bond angles within the LiO_4, FeO_4, and SiO_4 tetrahedra before and after Li removal for each polymorph. In the LiO_4 tetrahedra there is a large increase in the distortion of the shape of the tetrahedra after Li removal, which is especially pronounced in the β_{II} structure. The LiO_4 tetrahedra have weakly hybridized bonds, and they have the lowest energetic cost of distortion. The SiO_4 tetrahedra contain strong Si−O bonds which require considerable energy to become distorted. The SiO_4 distortion is most pronounced in the β_{II} structure after Li removal which partly explains why its energy is so high (Figure 2). It is of

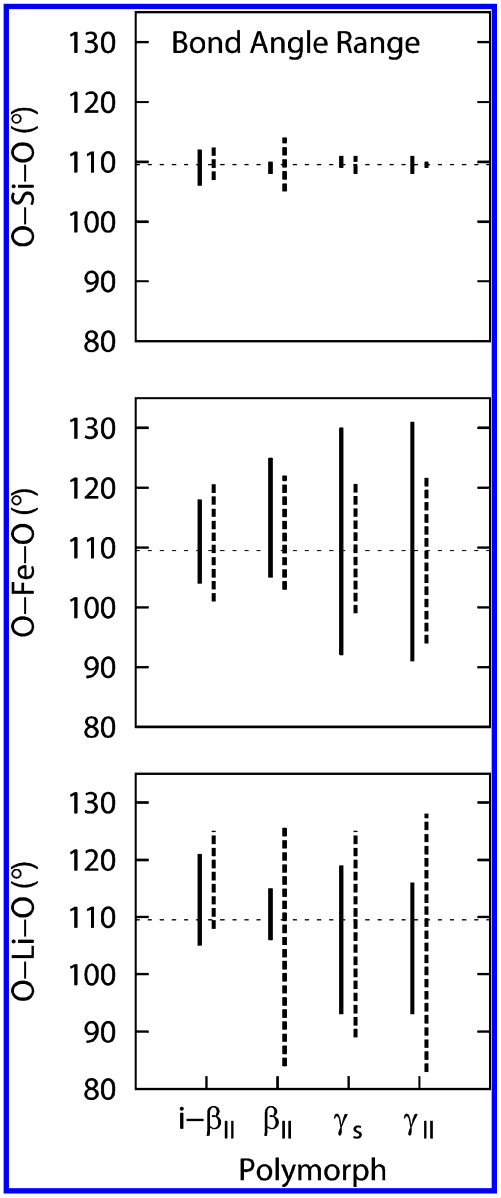

Figure 4. Range of bond angles in the LiO_4, FeO_4, and SiO_4 tetrahedra of the Li_2FeSiO_4 and delithiated $LiFeSiO_4$ structures (filled and dashed lines, respectively) as a measure of the tetrahedral distortion. The horizontal dashed line is the ideal tetrahedral angle.

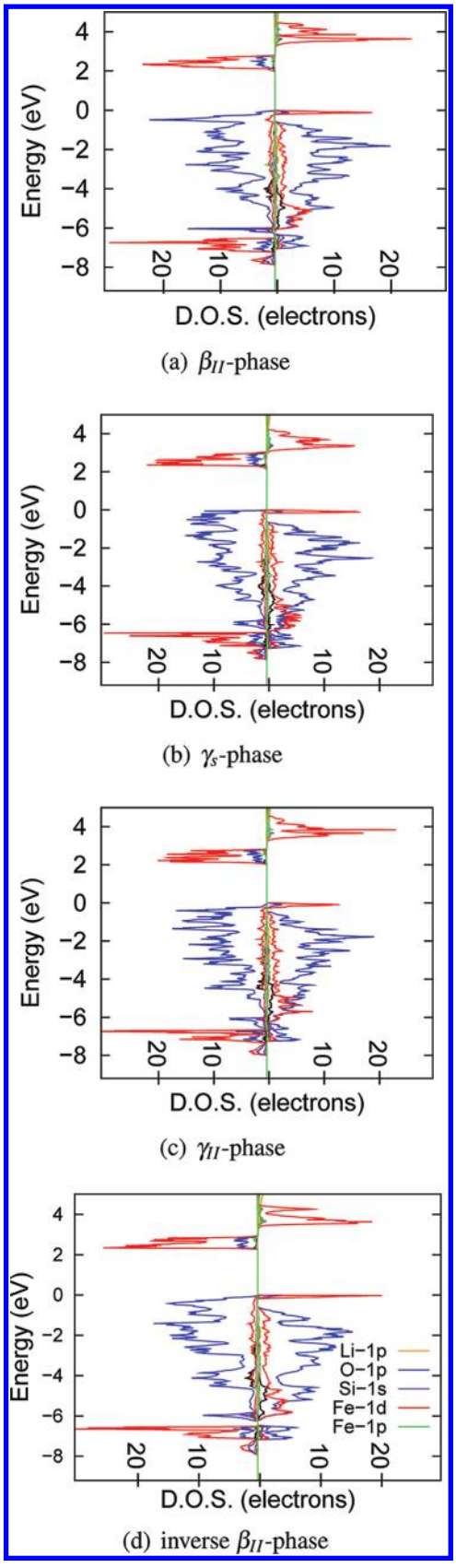

Figure 5. Electron density of states in the Li_2FeSiO_4 (left panel) and $LiFeSiO_4$ (right panel) state of each polymorph of lithium iron silicate.

dx.doi.org/10.1021/cm300749w | Chem. Mater. 2012, 24, 2155−2161

note that in the cycled (inverse-β_{II}) structure the level of distortion in all tetrahedra is not so different before and after Li removal, which may explain the small energy difference between Li_2FeSiO_4 and $LiFeSiO_4$ and the low cell voltage.

It appears that the ionic and covalent aspects of the structure compete in order to reduce the long-range electrostatic energy and the bond distortion energy. Cation repulsion acts to reduce the energy by maximizing the cation spacings by expanding the cell volume. The covalent hybridized bonds act to minimize the energy by preventing distortion of the tetrahedral symmetry.

One further aspect to consider is the electronic density of states of the four polymorphs, which we have calculated using a fine 10 × 10 × 10 mesh to extract the band structure non-self consistently from the electronic structure. The LINDOS program was then used to sum the band occupancies at each energy and produce the density of states presented in Figure 5. As found in previous work,[16,17,20] the spectra are dominated by the O 2p states and the Fe 3d states. The Fe 3d rehybridization is very evident as we move from Li_2FeSiO_4 to $LiFeSiO_4$. However, if we compare the four polymorphs in either the Li_2FeSiO_4 or $LiFeSiO_4$ states there are no significant differences between the DOS, and these will not make a large contribution to the cell voltage trends.

To summarize our findings, the observed cell voltages of the polymorphs of lithium iron silicate can now be rationalized in turn starting with the cycled structure.

[inverse-β_{II}: 2.76 V]: This polymorph has the highest energy as Li_2FeSiO_4 because it has the largest distortion in the SiO_4 tetrahedra, short O−O distances, and distorted LiO_4 tetrahedra. After delithiation to $LiFeSiO_4$, it undergoes a +5.6% volume expansion, giving it the largest cation−cation spacings of the four delithiated structures. Crucially this does not introduce any significant extra distortion into the tetrahedra. The energy change upon delithiation is the smallest of all the polymorphs and it has the lowest cell voltage. The phase transition into the inverse-β_{II} structure that occurs when the three as-prepared polymorphs are delithiated can be explained as maximizing the cation−cation spacings by adopting the mixed cation Li/Fe scheme.

[β_{II}: 3.10 V]: This polymorph is corner sharing like inverse-β_{II} and differs only in its cation ordering. Upon delithiation to $LiFeSiO_4$ the volume expansion is restricted to +4.2% by the large and energetically costly distortion which occurs in the SiO_4 and LiO_4 tetrahedra. The tetrahedral distortion and electrostatic repulsion in the system are both high in energy and in direct competition, resulting in the highest cell voltage of the four polymorphs.

[γ_s: 3.00 V]: The most covalent SiO_4 and O−O networks and the most ionic LiO_4 tetrahedra result in the lowest energy in the lithiated state of the four polymorphs. Low distortion in the SiO_4 tetrahedra is achieved by high distortion in the LiO_4 tetrahedra, which raises the energy less. After delithiation to $LiFeSiO_4$ the cell volume contracts by −1.5%, causing the Fe−Fe spacings to reduce, which together with the increased ionic nature of the Fe cores increases the total energy. It now also possesses the least ionic LiO_4 tetrahedra which are heavily distorted and energetically costly. All of these factors conspire to give the γ_s polymorph the second highest cell voltage.

[γ_{II}: 2.90 V]: This polymorph has shorter Li−Fe and Fe−Fe spacings than the γ_s polymorph when delithiated to $LiFeSiO_4$. What causes it to have a lower voltage than γ_s is that the LiO_4 tetrahedra are the most ionic out of the four polymorphs and their distortion is the least energetically unfavorable.

CONCLUSIONS

This systematic survey of the Li_2FeSiO_4 cathode material has used DFT methods to provide deeper understanding into the cell voltage changes and related structure−property relationships of the range of complex polymorphs, which complement related experimental and theoretical work.

The following key points emerge from our study. (1) We have been able to examine the energetics and cell voltages of the three as-prepared polymorphs (β_{II}, γ_s, and γ_{II}) versus the recently elucidated cycled structure (inverse-β_{II}). We see good agreement with the measured values of the voltage change (ΔV vs Li+/Li) upon cycling across these polymorphs, in which we find ΔV of −0.30 V, −0.24 V, and −0.18 V for β_{II}, γ_s, and γ_{II}, respectively. (2) The trends in cell voltage have been correlated to the change in energy upon delithiation from Li_2FeSiO_4 to $LiFeSiO_4$ in which the cation−cation electrostatic repulsion competes with distortion of the tetrahedral framework. The results suggest that the structural phase change into the cycled structure occurs upon lithium extraction because it has a particular cation arrangement that allows the cation−cation spacings to be maximized without significant distortion of the corner-sharing tetrahedra. (3) The calculated Si−O bond lengths show relative invariance with Li extraction, whereas the mean Fe−O bond length shortens significantly from Li_2FeSiO_4 to $LiFeSiO_4$, consistent with the oxidation of Fe^{2+} to Fe^{3+}. The redox couple does not seem to contribute to the trend in voltage differences across the polymorphs, with the Fe−O bond lengths remaining uniform for the structures in both Li_2FeSiO_4 and $LiFeSiO_4$ states. The electronic densities of states are also relatively invariant across the polymorphs and do not seem to contribute significantly to the trend in voltage changes.

In general, these findings suggest that structure−property features for high cell voltages in these iron−silicate cathode materials should include not only the formal valence state of Fe but also the change in energy upon delithiation, which is influenced by the balance between the cation−cation repulsion and the distortion of the covalent tetrahedral framework, which is, in turn, influenced by the polymorph structure.

Further studies to investigate these structural properties are warranted, for example, directed toward the synthesis of a Li_2FeSiO_4 polymorph that is stable from the outset to avoid the electrochemistry changing on cycling.

ASSOCIATED CONTENT

Supporting Information

Tables S5−S9 showing lattice parameters and relative total energies, atomic positions, and Mulliken atomic charges (PDF). This material is available free of charge via the Internet at http://pubs.acs.org.

AUTHOR INFORMATION

Corresponding Author

*E-mail: m.s.islam@bath.ac.uk.

Notes

The authors declare no competing financial interest.

ACKNOWLEDGMENTS

This work was funded by the EPSRC Supergen programme and made use of the high-performance computing service HECToR, via the HPC Materials Chemistry Consortium. The LINDOS code was written by A. J. Morris and C. J. Pickard at University College London.

REFERENCES

(1) Nyten, A.; Abouimrane, A.; Armand, M.; Gustafsson, T.; Thomas, J. O. *Electrochem. Commun.* **2005**, *7*, 156−160.
(2) Islam, M. S.; Dominko, R.; Masquelier, C.; Sirisopanaporn, C.; Armstrong, A. R.; Bruce, P. G. *J. Mater. Chem.* **2011**, *21*, 9811−9818.
(3) Dominko, R.; Conte, D.; Hanzel, D.; Gaberščcek, M.; Jamnik, J. *J. Power Sources* **2008**, *178*, 842−847.
(4) Dominko, R. *J. Power Sources* **2008**, *184*, 462−468.
(5) Nishimura, S.-i.; Hayase, S.; Kanno, R.; Yashima, M.; Nakayama, N.; Yamada, A. *J. Am. Chem. Soc.* **2008**, *130*, 13212−13213.
(6) Boulineau, A.; Sirisopanaporn, C.; Dominko, R.; Armstrong, A. R.; Bruce, P. G.; Masquelier, C. *Dalton Trans.* **2010**, *39*, 6310−6316.
(7) Sirisopanaporn, C.; Boulineau, A.; Hanzel, D.; Dominko, R.; Budic, B.; Armstrong, A. R.; Bruce, P. G.; Masquelier, C. *Inorg. Chem.* **2010**, *49*, 7446−51.
(8) Nyten, A.; Kamali, S.; Haggstrom, L.; Gustafsson, T.; Thomas, J. O. *J. Mater. Chem.* **2006**, *16*, 2266−2272.
(9) Sirisopanaporn, C.; Masquelier, C.; Bruce, P. G.; Armstrong, A. R.; Dominko, R. *J. Am. Chem. Soc.* **2011**, *133*, 1263−1265.
(10) Armstrong, A. R.; Kuganathan, N.; Islam, M. S.; Bruce, P. G. *J. Am. Chem. Soc.* **2011**, *133*, 13031−13035.
(11) Muraliganth, T.; Stroukoff, K. R.; Manthiram, A. *Chem. Mater.* **2010**, *22*, 5754−5761.
(12) Gong, Z. L.; Li, Y. X.; He, G. N.; Li, J.; Yang, Y. *Electrochem. Solid State Lett.* **2008**, *11*, A60−A63.
(13) Zaghib, K.; Salah, A. A.; Ravet, N.; Mauger, A.; Gendron, F.; Julien, C. *J. Power Sources* **2006**, *160*, 1381−1386.
(14) Dominko, R.; Bele, M.; Gaberščcek, M.; Meden, A.; Remškar, M.; Jamnik, J. *Electrochem. Commun.* **2006**, *8*, 217−222.
(15) de Dompablo, M. A.; Armand, M.; Tarascon, J.; Amador, U. *Electrochem. Commun.* **2006**, *8*, 1292−1298.
(16) Zhong, G.; Li, Y.; Yan, P.; Liu, Z.; Xie, M.; Lin, H. *J. Phys. Chem. C* **2010**, *114*, 3693−3700.
(17) Larsson, P.; Ahuja, R.; Nytén, A.; Thomas, J. O. *Electrochem. Commun.* **2006**, *8*, 797−800.
(18) Kokalj, A.; Dominko, R.; Mali, G.; Meden, A.; Gaberscek, M.; Jamnik, J. *Chem. Mater.* **2007**, *19*, 3633−3640.
(19) Yabuuchi, N.; Yamakawa, Y.; Yoshii, K.; Komaba, S. *Dalton Trans.* **2011**, *40*, 1846−1848.
(20) Wu, S.; Zhu, Z.; Yang, Y.; Hou, Z. *Comput. Mater. Sci.* **2009**, *44*, 1243−1251.
(21) Saracibar, A.; Van der Ven, A.; Arroyo-de Dompablo, M. E. *Chem. Mater.* **2012**, *24*, 495−503.
(22) Zhou, F.; Cococcioni, M.; Marianetti, C. A.; Morgan, D.; Ceder, G. *Phys. Rev. B* **2004**, *70*, 235121.
(23) Zhou, H.; Upreti, S.; Chernova, N. A.; Hautier, G.; Ceder, G.; Whittingham, M. S. *Chem. Mater.* **2011**, *23*, 293−300.
(24) Hautier, G.; Jain, A.; Chen, H.; Moore, C.; Ong, S. P.; Ceder, G. *J. Mater. Chem.* **2011**, *21*, 17147−17153.
(25) Armstrong, A. R.; Lyness, C.; Panchmatia, P. M.; Islam, M. S.; Bruce, P. G. *Nat. Mater.* **2011**, *10*, 223−229.
(26) Kuganathan, N.; Islam, M. S. *Chem. Mater.* **2009**, *21*, 5196−5202.
(27) Gardiner, G. R.; Islam, M. S. *Chem. Mater.* **2010**, *22*, 1242−1248.
(28) Fisher, C. A. J.; Hart Prieto, V. M.; Islam, M. S. *Chem. Mater.* **2008**, *20*, 5907−5915.
(29) Islam, M.; Driscoll, D.; Fisher, C.; Slater, P. *Chem. Mater.* **2005**, *17*, 5085−5092.
(30) Clark, S.; Segall, M.; Pickard, C.; Hasnip, P.; Probert, M.; Refson, K.; Payne, M. *Z. Kristallogr.* **2005**, *220*, 567−570.
(31) Wang, Y.; Perdew, J. P. *Phys. Rev. B* **1991**, *44*, 13298−13307.
(32) Zhou, F.; Cococcioni, M.; Kang, K.; Ceder, G. *Electrochem. Commun.* **2004**, *6*, 1144−1148.
(33) Ceder, G.; Aydinol, M.; Kohan, A. *Comput. Mater. Sci.* **1997**, *8*, 161−169.
(34) Arrouvel, C.; Parker, S. C.; Islam, M. S. *Chem. Mater.* **2009**, *21*, 4778−4783.
(35) Goodenough, J. B.; Kim, Y. *Chem. Mater.* **2010**, *22*, 587−603.
(36) Segall, M.; Shah, R.; Pickard, C.; Payne, M. *Phys. Rev. B* **1996**, *54*, 16317−16320.